Food Structure 46 (2025) 100492

Contents lists available at ScienceDirect

Food Structure

journal homepage: www.elsevier.com/locate/foostr

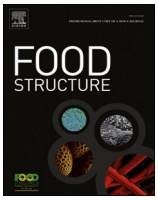

Consumer preferences of plant-based minced meat analogs: Linking physico-chemical properties, structural features, and sensory attributes

Jaqueline Auer [a,*,1], Ansung Kim [b,*,1], Sarah Heupl [c], Mihaela Mihnea [b], Åsa Öström [b], Jun Niimi [d], Maud Langton [a]

[a] Department of Molecular Sciences, Swedish University of Agricultural Sciences, Uppsala 750 07, Sweden
[b] School of Hospitality, Culinary Arts and Meal Science, Örebro University, Örebro 701 82, Sweden
[c] University of Applied Sciences Upper Austria, Stelzhamerstraße 23, Wels 4600, Austria
[d] RISE Research Institutes of Sweden, Division of Bioeconomy & Health, Product Design, Sweden

ARTICLE INFO

Keywords:
Fiber structure
Sensory properties
Consumer
Food microstructure, Computed tomography (CT)

ABSTRACT

Plant-based food products offer a sustainable option for consumers seeking to reduce meat intake while maintaining the sensory satisfaction similar to conventional meat. However, the products in question are still unsatisfactory, and simulating the sensory properties that consumers find palatable remains significantly challenging. This study investigated the physicochemical and sensory properties of plant-based minced meat analogs, with an emphasis on texture (including texture profile analysis (TPA), liquid holding capacity (LHC), and fiber orientation) and appearance (color and particle size). Four commercial plant-based products were evaluated: two soy-based (Soy I and Soy II) and two pea-based (Pea I and Pea II) to elucidate the relationship between microstructural features and consumer sensory perception. TPA results indicated that soy-based products exhibited significantly higher hardness, gumminess, and chewiness compared to pea-based products. LHC and colour analyses revealed notable differences among the samples: Pea I showed the lowest mass loss, indicating superior water retention, while Pea II displayed pronounced red and yellow colour values. Particle size analysis indicated that Pea II and Soy I contained larger and more heterogeneous particles, whereas Soy II was characterized by smaller and more uniform particulates. Further, fiber orientation analysis revealed that Soy II exhibited more aligned fiber structures, which may contribute to its higher mechanical resistance and firmness. Sensory evaluation indicated consumer preference for Soy II, which was perceived as chewier and more rubbery in texture. The overall pattern from sensory evaluation was consistent with instrumental measurements, underscoring the utility of structural and mechanical analyses in predicting consumer acceptance.

1. Introduction

The growing interest in meat analogs is driven by environmental (Mikael, 2020; Xu et al., 2021), ethical (Fehér et al., 2020), and health-related (Satija & Hu, 2018) concerns associated with traditional meat production and consumption. A primary objective of meat analogs is to replicate the sensory characteristics of meat to appeal to a broad range of consumers (Fiorentini et al., 2020; Giacalone et al., 2022; He et al., 2020). There are studies which suggest that plant-based products should be designed to closely match the quality attributes of animal-based products because consumer familiarity with these attributes can facilitate a smoother transition to alternatives (Hoek et al., 2011; H. Zhou et al., 2022). In particular, studies have reported insufficient quality in texture, taste, and appearance as key barriers to consumer acceptance of meat analogs (Kerslake et al., 2022; Michel et al., 2021). For example, Sogari et al. (2023) conducted a consumer sensory evaluation of meat analogs in burger patty form. Their findings revealed that consumers were able to distinguish meat analog patties from beef patties based on taste, texture, and appearance, and that these attributes were key factors influencing product liking or disliking. Moreover, consumers expressed a preference for meat-like texture attributes (e.g. juiciness and chewiness) in their ideal plant-based minced meat analogs (Kim et al., 2024). However, other research suggests that resemblance to meat is not always necessary for consumer acceptance. For instance,

* Corresponding authors.
E-mail addresses: jaqueline.auer@slu.se (J. Auer), ansung.kim@oru.se (A. Kim).
[1] authors contributed equally

https://doi.org/10.1016/j.foostr.2025.100492
Received 4 June 2025; Received in revised form 25 November 2025; Accepted 29 November 2025
Available online 3 December 2025

Godschalk-Broers et al. (2022) found that texture parameters do not necessarily need to mimic those of real meat to achieve consumer appreciation. Similarly, Niimi et al. (2022) demonstrated that the attributes driving consumer liking of meat analogs in Bolognese sauce form were not necessarily related to meat-like qualities. In fact, one of the plant-based meat analogs was preferred over its conventional meat counterpart. These findings highlight that consumer preferences for meat analogs could vary in their expectations of meat resemblance. Therefore, it remains unclear to how closely meat analogs should mimic conventional meat products (Wild, 2016; H. Zhou et al., 2022).

To identify the consumer's preferred characteristics, it is necessary to combine sensory research, physiology studies, and food physicochemical characteristics (Wilkinson et al., 2000). While there is a lack of standardized methods available to characterize the physico-chemical properties of food products (Grossmann et al., 2021; McClements et al., 2021), attributes such as color, shape, water, oil holding capacity, and texture have been identified as important factors for the initial screening of different products (Schreuders et al., 2021; H. Zhou et al., 2022). In addition, the structural characteristics of food play a vital role in shaping overall sensory perception. Structure refers to the physical organization and arrangement of components within a food matrix at different scales, from the molecular to the macroscopic level (Damez & Clerjon, 2008). Texture, whereas, describes the sensory perception that arises from this structure during handling, chewing, and swallowing (Nishinari & Fang, 2018). Thus, while structure can be objectively characterized through analytical or imaging techniques, texture reflects the subjective experience of that structure as perceived by the consumer.

Given the complex composition of food products, there is an increasing need for advanced methods that can characterize their three-dimensional structure and translate visual information into quantitative data (Wilkinson et al., 2000). Accordingly, various imaging techniques such as electron microscopy, confocal laser scanning microscopy (Godschalk-Broers et al., 2022), and Computed Tomography (CT) combined with image analyses are increasingly applied to characterize the 3D structure of meat analogs (Dekkers et al., 2018; Fu et al., 2023).

Image analyses are often used to determine features such as pore structures (Schreuders et al., 2019) pore volume, and size distributions (Schoeman et al., 2016), whereas there has been less focus on the characterization of fibers and fiber structures. Fiber characterization tools are widely utilized in material sciences to analyze the fiber structure in fiber-reinforced concrete (B. Zhou & Uchida, 2017) or polymers (Maurer et al., 2024). Although image analysis has been successfully used to describe fiber characteristics in meat analogs (Wu et al., 2024), the potential of fiber characterization tools for analyzing food microstructures remains underexplored, as most studies primarily focus on 2D characterization.

This study aimed to investigate the possibility of using Computed Tomography (CT) and fiber characterization, together with other measurements, such as color, shape, liquid holding capacity, and texture, to identify structural features that may explain consumer preferences of meat analogs. Therefore, the microstructure of four different minced meat analogs that are currently available on the Swedish market are characterized and the resulting structural features are linked to sensory perception. The findings will enable us to draw conclusions on which structural properties lead to textural appreciation by consumers (omnivores and vegans/vegetarians), with a main focus on the general textural attributes that are valued, without directly comparing them to real meat.

2. Material and methods

2.1. Sample and sample preparation

Four commercial plant-based minced meat analogs were included in this study (Table 1), two soy-based (Soy I and Soy II) and two pea-based (Pea I and Pea II). Soy and pea were chosen because they are commonly used in meat analogs. Furthermore, products with similar fat and protein content were selected to focus on differences in texture rather than variations in composition. The products were purchased at local supermarkets in Uppsala and Gothenburg, Sweden.

Table 1
Description of the samples, status at which each product was sold in retail, and each of their ingredient lists as provided by the manufacturers.

Sample name	Status	Ingredients
Soy I	Frozen	Water, SOY PROTEIN (23 %), rapeseed oil, methylcellulose (E461), salt, onion powder, tomato powder, caramelized sugar, garlic powder, black pepper
Soy II	Frozen	Water, SOY PROTEIN (26 %), rapeseed oil, onions, salt, spices, natural flavors, caramelized sugar
Pea I	Frozen	Water, PEA PROTEIN (23 %), rapeseed oil, apple extract, natural flavors, salt, methylcellulose (E461)
Pea II	Fresh	Water, PEA PROTEIN (25 %), rapeseed oil, thickener (E461), natural aroma, spices, spice extract, salt, vinegar, beetroot powder

The samples were prepared identically for both the physico-chemical analysis and the consumer sensory evaluation. With the exception of Pea II, which was a fresh product stored in a refrigerator (4℃), all of the samples were frozen products stored in a freezer (-18℃). Prior to the cooking process, the frozen samples were thawed overnight at 4℃. Afterward, 600 g of each product was stir-fried in 30 g rapeseed oil on medium heat for 8 min. The cooked samples were cooled to room temperature (21℃) and were portioned out into servings of approximately 20 g each in transparent plastic containers (60 ml) with lids for the consumer study. The samples were stored at 4℃ until being handed out to consumers or being performed physco-chemical analyses. All analyses were performed at room temperature on the stir-fried products to ensure that all consumers evaluated the samples under consistent conditions, thereby minimizing external influences on sensory perception. A visual overview of the final products is provided in Figure A1

2.2. Physical-chemical analysis

2.2.1. Texture profile analysis

The texture profile analysis (TPA) (Bourne, 1978) was performed using a Stable Microsystem (TA-HDi, Surrey, UK) equipped with a 50 kg load cell and a 36 mm cylindrical aluminum probe. The samples were placed in a plastic beaker (⌀ 40 mm) and filled to a height of 30 mm. The samples were then compressed to 50 % strain (trigger force 15 g) with a test speed of 2 mm/s. The waiting time between the first and second compression was 5 sec (H. Zhou et al., 2022). Following this, four textural parameters were computed: Hardness (N): the highest force recorded during the first compression; Springiness (%): The ratio of the recovery of the product to its original height; Gumminess (N): hardness × cohesiveness; Chewiness (N): Hardness × Cohesiveness × Springiness. All the TPA measurements were replicated 5 times.

2.2.2. Liquid holding capacity and dry matter content

To determine the liquid-holding capacity (LHC) of the cooked products low-speed centrifugation was used (Zhang et al., 1995) to quantify the mass loss (H. Zhou et al., 2022). Approximately 1 g of product was placed in a 2 ml Spin-X centrifuge tube filter with a pore size of 0.22 μm (Corning® Costar® Spin-X®, CLS8161). The samples were each centrifuged for 300 sec at six settings: 200, 500, 1000, 1500, 2000, and 2500 × g (Eppendorf, Centrifuge 5430 R). After each centrifugation step the samples were weighed and the mass loss was recorded in % w/w. Thereby different centrifugation speeds were chosen to assess the product's ability to retain both loosely and tightly bound water and other fluids under different stress conditions. Furthermore, the moisture matter content was determined to account for variations in initial water content between samples. Dry matter was

measured according to AOAC Official Method 934.01 by drying the samples to constant weight (>20 h) in a convection oven (Model 2000655, J.P. Selecta, Barcelona, Spain) at 105 °C. Both analyses were performed in triplicate.

2.2.3. Colour measurement

The color of the products was measured using a colorimeter (CR-300, Minolta, Japan). The results are expressed as CIE-lab parameters L*, a*, and b*, where L* refers to the lightness of the sample (0 = black and 100 = white), a* to the greenness (-a*)/redness (+a*), and b* to the blueness (-b*)/ yellowness (+b*). For the measurement, the built-in light source was placed in the sample and the L*a*b values were recorded in 8 different regions of each sample. The hue angle H^*; Eq. (1), chroma C^*; Eq.(2), and total color change ΔE^*; Eq. (3) were calculated from the average L*, a*, and b* values and used to describe the color differences of the products. All measurements were performed in triplicate.

$$H^* = \tan^{-1}\left(\frac{b^*}{a^*}\right) \quad (1)$$

$$C^* = \sqrt{(a^*)^2 + (b^*)^2} \quad (2)$$

$$\Delta E^* = \sqrt{(\Delta L^*)^2 + (\Delta a^*)^2 + (\Delta b^*)^2} \quad (3)$$

2.2.4. Projected particle area

To determine the projected particle area, ImageJ 1.53c (Wayne Rasband, National Institutes of Health, USA) was used. For each sample, three 8-bit images were taken, with the products spread evenly on a white surface for analysis. The images were captured using a 12-megapixel digital camera (4032 × 3024 pixels) under uniform light conditions and at a fixed distance from the sample. To smooth out inhomogeneity, a Gaussian Blur filter (sigma value 2) was applied. The image was converted into a binary image (upper threshold 0, lower threshold 15 %), and the watershed method was used to separate objects. Falsely separated objects were manually excluded, and 255–541 individual particles were used to describe the projected particle area.

2.2.5. Fiber orientation

To determine the fiber orientation using Light microscopy the stir-fried samples were frozen in liquid nitrogen and cut into 25 μm sections using a cryostat at −20℃ (Leica CM1850, Wetzlar, Germany). The sections were subsequently examined under a microscope (Nikon, Eclipse Ni–U microscope, Tokyo, Japan) equipped with a 40 × (0.75 NA) objective. Images were captured with a Nikon Digital Sight DS-Fi2 camera (Nikon, Tokyo, Japan) with 0.12 μm/pixel. The micrographs were then transformed into binary images (Threshold ISO 50) using ImageJ 1.53c and the orientation of the fibers was evaluated for every 10 pixels using the plugin, orientationJ (Rezakhaniha et al., 2012). The interval of 10 pixels was chosen to balance computational efficiency with adequate spatial resolution for reliable detection of local fiber orientation. Images were binarized prior to analysis to enhance contrast and reduce noise, enabling clearer detection of fiber boundaries. An overview of the image analysis is provided in the appendix (Figure A2).

To characterize the 3D fiber orientation in each product the samples were frozen in liquid nitrogen and freeze-dried (Martin Christ, Epsilon 2–6D LSC Plus, Germany). The dried samples were then scanned using the RX Solutions Easytom 160 (RX Solutions, Franc) equipped with a flat panel detector. The samples were scanned with 60 kV and a current of 111 μA. The number of projections was 3008 and the voxel size was 9 μm. The reconstructed 3D datasets were processed in VGSTUDIO MAX 2024.1 to quantify fiber orientation. Two complementary analysis modes were employed: (I) *plane projection*, which visualizes the predominant alignment of fibers within specific cross-sectional planes, and (II) *space orientation*, which quantifies the global 3D distribution of fiber directions. The integration radius was set to 1 voxel to capture local orientation variations, and the surface determination tool was applied to accurately define the boundaries of the fibrous structures.

2.3. Consumer sensory evaluation

A total of 99 consumers (66 female; 33 male) participated in the sensory evaluation, with more than half identifying as omnivores, and the remainder as flexitarians (10 %), pescatarians (8 %), vegetarians (17 %), and vegans (9 %). In relation to the consumption of meat analogs, 27 per cent of consumers reported consuming such products more than once a week, whereas 20 per cent had never tried meat analogs or had only tried them once. However, more than half of the consumers reported infrequent consumption of meat analogs, indicating intake of less than once a week or less than once a month. The consumer study was conducted as a home-use test due to COVID-19 restrictions at the time of testing. Therefore, consumers were required to collect a sensory evaluation package from a centralized location. The package contained stir-fried samples, which were individually packaged in transparent plastic containers that were labeled with a random three-digit code and contained approximately 20 g of each sample. The package also included serviettes, cutlery, plain crackers, printed lists of attributes with definitions, and instructions on evaluation protocols, including a QR code link to access the questionnaire. Consumers were instructed to keep the package in the refrigerator until 30 min before the evaluation and to evaluate the samples within 24 h of collection. The consumers first evaluated the products' hedonic values (appearance, aroma, taste, texture, and overall) on a 9-point hedonic scale. They then evaluated the intensities of sensory attributes using a 5-point rate-all-that-apply (RATA) intensity scale (Table A1). Sensory characteristics assessed by consumers consisted of 39 attributes including appearance (7), aroma (8), taste (14), texture (8), and after-taste/texture (2) modalities, which were pre-generated by six experienced sensory panelists prior to the consumer test (Table A2). All involved consumers provided informed consent and were compensated with a 250 SEK gift card for their participation upon completion. Data was collected through consumers' smartphones using RedJade® Sensory Solutions (Silicon Valley, CA, USA). The study was carried out in accordance with the Declaration of Helsinki (World Medical Association, 2013) and approved by the Department of Material and Surface Design at RISE Research Institutes of Sweden. Personal data was collected and handled in accordance with the General Data Protection Regulation (GDPR) (EU) 2016/679. For further study details, see Kim et al. (2024).

2.4. Data analysis

Results for the structural characterization i.e. TPA, LHC, moisture content, color, and particle size measurements are presented as means and standard deviations. One-way analysis of variance (ANOVA) followed by Fisher's least significant difference (LSD) at a confidence interval of 95 % was used to compare the means. For the fiber analyses, one representative subvolume was selected for the 2D image analysis, corresponding to an area of 3130 × 2350 μm, extracted from the central region of each section to ensure a representative overview of the internal structure. In contrast, for the 3D CT analysis, the entire scanned volume of each sample was analyzed. In sensory data analysis, the following data from the four samples was relevant for this study: hedonics of appearance, texture, and overall intensities of attributes from appearance (homogeneous pieces, homogeneous color, moist, brown color, red color, grainy, and fibrous) and texture (rubbery, juicy, oily, grainy, fibrous, chewing resistance, mealy, and remaining after texture) modalities. As the focus of this study was on texture and modalities relevant for surface texture of the samples, other modalities such as aroma and taste (including flavor) were not subjected to data analysis. Moreover, because the sensory data was not normally distributed, Kruskal-Wallis tests were conducted with Dunn-Bonferroni post-hoc tests to

investigate the differences in sensory attributes by samples. Additionally, the effect sizes (Cohen's *d*), which demonstrate the magnitude of a statistical significance, were calculated (Lenhard & Lenhard, 2022). The established criteria for interpreting Cohen's d defines the magnitude of observed effects as follows: no effect (0–0.1), small effect (0.2–0.4), moderate effect (0.5–0.7), and large effect (0.8 or above). Principal component analysis (PCA) was used to project the samples as scores separately in relation to the physico-chemical data and sensory data (both as loadings). The hedonic value was included as supplementary data in the analysis of sensory data. To obtain further insights into the relationship between the physico-chemical data and sensory data in terms of sample projections, multiple factor analysis (MFA) was employed together with hedonic value as supplementary data in the analysis. The statistical analyses ($p > 0.05$) of the physico-chemical data and sensory data were conducted using R (Version 4.3.0, RStudio Inc., MA, USA) and XLstat (Version 2022.2.1, Addinsoft, New York, USA), respectively.

3. Results and discussion

The results summarize the findings from various physico-chemical analyses conducted on the four minced meat analogs, with each analysis discussed individually. Given the limited research available on plant-based minced meat, the discussion also includes comparisons with animal-based minced meat, as meat analogs are designed to closely replicate the appearance and structure of specific meat products. Finally, the physico-chemical properties are linked to consumer testing, aiming to identify the characteristics that contribute to overall preference and should be prioritized in the future development of plant-based foods.

3.1. Texture profile analysis

The results from the texture profile analysis (TPA) of the different minced meat analogs are displayed in Table 2. Soy II showed the highest hardness followed by Soy I. The two pea products showed a significantly ($p < 0.001$) lower hardness than the two soy products, while no significant difference was found between the two pea products. The gumminess and chewiness of the two soy products was significantly ($p < 0.001$) higher than those in the pea products, with Soy II exhibiting the highest gummies. In contrast, no significant differences were found in the overall springiness of the products ($p < 0.355$).

The general differences in texture could be a result of differences in the overall structure and composition e.g. fat and water content (Godschalk-Broers et al., 2022) or whether soy or pea proteins were used in the product. Previous results from Wang et al. (2022) revealed that the textural properties of extrudates from soy protein isolate can differ from extrudates made from pea protein isolate. The textural differences have been identified as a result of differences in microstructure in which soy protein isolate created a more compact structure than the extrudates made from pea protein isolate (Wang et al., 2022). When comparing the texture profile with the structural characteristics of the products (Fig. 3) a similar trend can be observed for the Soy II product. Based on the micrographs this product showed a compact structure which could lead to a harder and more springy texture. However, the Soy I product exhibited a less compact structure and a comparably high hardness which could indicate that the microstructure is only one factor that influences the hardness of the product. Further, the presence of components such as starch and dietary fiber in varying concentrations has been shown to influence the structure of minced meat (Y. S. Choi et al., 2011; Özer & Seçen, 2018) and meat analogs (Guyony et al., 2022; Ramos Diaz et al., 2022; Wi et al., 2020). Although products with similar ingredients and nutritional composition were chosen for this study to primarily focus on structure, small differences in preparation and ingredients, e.g., the amount of methylcellulose used, can influence the textural properties (Bakhsh et al., 2021).

Table 2
Texture profile analysis (TPA) results from the different products containing primary parameters (hardness, springiness) and secondary parameters (gumminess, chewiness).

Product	Hardness (N)	Springiness (%)	Gumminess (N)	Chewiness (N)
Soy I	40.5 ± 3.5^{b}	49.7 ± 3.4	25.1 ± 2.4^{b}	12.6 ± 2.0^{a}
Soy II	55.5 ± 7.8^{a}	45.8 ± 3.9	29.7 ± 4.6^{a}	13.7 ± 2.9^{a}
Pea I	28.3 ± 1.8^{c}	47.5 ± 5.5	15.7 ± 1.0^{c}	7.4 ± 1.0^{b}
Pea II	22.8 ± 3.8^{c}	43.5 ± 5.9	12.6 ± 2.2^{c}	5.5 ± 1.2^{b}
P - value	< 0.001	0.355	< 0.001	< 0.001

Results are presented as mean ± standard deviation; different superscript letters indicate significant differences according to Fisher's least significant difference ($p < 0.001$).

3.2. Liquid-holding capacity

The liquid-holding capacity (LHC) of meat and meat analogs is typically related to the perceived juiciness of a product (Aaslyng et al., 2003; H. Zhou et al., 2022). In this study, the LHC was evaluated indirectly by measuring the mass loss (%) after centrifugation, where a lower mass loss indicates a higher LHC. The mass loss of the different meat analogs is shown in Fig. 1. Using low centrifugal force (200 × g), significant differences ($p < 0.05$) between the different products were found, with Pea II showing the highest mass loss (1.4 ± 0.4 %) and both Soy I (0.6 ± 0.1 %) and Pea I (0.4 ± 0.2 %) showing the lowest mass loss. At high centrifugal force, (2500 × g) no significant difference was found between Soy I, Soy II, and Pea II. However, Pea I showed a significantly ($p < 0.05$) lower mass loss compared to the other products.

These differences at low centrifugal force partly explain the textural differences observed between Soy I and Soy II. Soy II exhibited a slightly higher mass loss than Soy I, indicating a lower water-binding capacity and suggesting that its structure retained water less effectively under mild stress conditions. This aligns with the higher hardness previously measured for Soy II. Importantly, Soy II was the only product formulated without methylcellulose, an ingredient known to markedly improve water retention through thermo-reversible gelation during heating (Bakhsh et al., 2021). The absence of methylcellulose, therefore, potentially provides a mechanistic explanation for the reduced LHC and increased firmness of Soy II.

To further contextualize these findings, the moisture content of the products was also determined (Table A3). Although all products showed similar moisture levels (ranging from 51.5 % to 53.1 %), Soy II had a

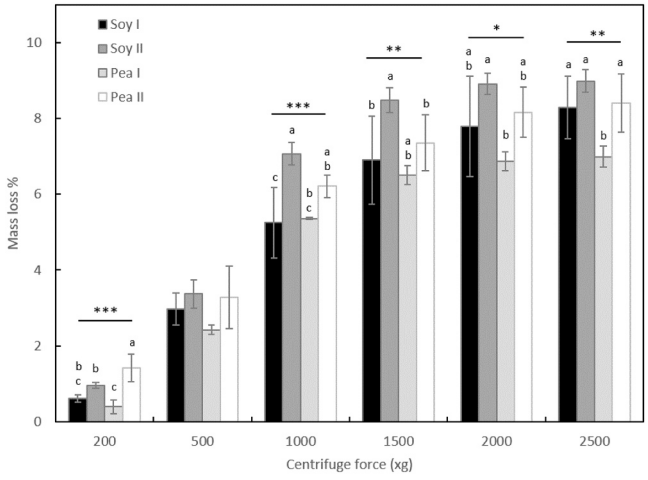

Fig. 1. Mass loss of the analyzed products at different centrifugal forces presented as mean ± standard deviation. Different superscript letters indicate significant differences according to Fisher's least significant difference ($p < 0.05$*; $p < 0.01$**; $p < 0.001$***).

slightly higher moisture content than Soy I. Despite this, Soy II exhibited a marginally higher mass loss during centrifugation, suggesting a lower water binding capacity relative to Soy I. This indicates that differences in LHC cannot be explained by initial moisture levels alone but rather by how water is structurally retained within the matrix. Since lower LHC and reduced water binding typically correspond to higher product firmness, this observation aligns with the higher hardness measured for Soy II. Conversely, Pea I, which exhibited both low mass loss and one of the highest moisture contents, demonstrates strong water retention, supporting its lower measured hardness.

The LHC of a product is dependent on various factors including the amino acid composition, conformation of proteins (Lam et al., 2018), and the microstructure of the product. Thereby, meat analogs with a denser structure have shown a higher LHC compared to more open and porous structures (Kaleda et al., 2021). The LHC can also be influenced by the addition of carrageenan (Candogan & Kolsarici, 2003), methylcellulose (Bakhsh et al., 2021), lecithin, oil, or water to the product (Wi et al., 2020). Methylcellulose, in particular, contributes to improved water retention and firmness through thermo-reversible gelation upon heating. When heated, it forms a gel network that enhances cohesion, reduces fluid loss, and strengthens the overall structure, which can increase hardness and chewiness as measured by texture profile analysis (Bakhsh et al., 2021). Therefore, the presence and concentration of methylcellulose can significantly influence the mechanical properties of meat analogs, such as hardness and gumminess, by stabilizing the internal matrix during cooking. However, beyond understanding the factors influencing LHC, it remains equally important to determine how these differences are perceived by consumers.

3.3. Color measurement

The results from the color measurements are shown in Table 3. Based on these results Pea II showed a significant ($p < 0.05$) higher lightness (L*), redness (a*), and yellowness (b*) compared to the other products. Further, Pea II showed the lowest hue angle and highest chroma value indicating a more reddish color with higher saturation. Contrastingly, Pea I and Soy I both displayed the lowest lightness while Soy II resulted in the lowest redness (a*) and yellowness (b*). Based on the hue angle and chroma value Soy II also showed a less pure reddish color (more closely resembling orange) with lower saturation than Pea II.

Based on the calculated total color difference as ΔE* pairwise between samples (Table 4), Soy II and Pea II showed the highest difference and Soy I and Pea I the lowest. The differences in perceivable color can be classified as very distinct (ΔE* > 3), distinct (1.5 < ΔE* < 3), and small difference (1.5 < ΔE*) (Adekunte et al., 2010; Pathare et al., 2013). Therefore, aside from Soy I and Pea I all products show distinct differences that are perceivable by the human eye.

Table 3
L* a* b* values of the different products with L* indicating the lightness, a* the green-red axes, and b* the blue and yellow axes. The chroma value indicates the degree of saturation of the color whereas the hue angle is used to locate colors in a circle where an angle of 0° or 360° represents red hue, while angles of 90°, 180°, and 270° represent yellow, green and blue hues.

Product	L*	a*	b*	H*	C*
Soy I	38.2 ± 1.4^{bc}	9.2 ± 0.4^{b}	34.1 ± 1.0^{b}	75.0 ± 0.8^{b}	35.4 ± 0.95^{b}
Soy II	39.3 ± 1.1^{b}	5.0 ± 0.5^{c}	31.3 ± 0.7^{c}	80.9 ± 1.0^{a}	31.7 ± 0.7^{c}
Pea I	37.5 ± 2.6^{c}	8.6 ± 1.6^{b}	33.4 ± 1.5^{b}	75.6 ± 2.9^{b}	34.5 ± 1.3^{b}
Pea II	44.6 ± 1.6^{a}	13.9 ± 0.9^{a}	37.9 ± 1.1^{a}	69.9 ± 1.1^{c}	40.3 ± 1.2^{a}
p-value	< 0.001	< 0.001	< 0.001	< 0.001	< 0.001

Different superscript letters indicate significant differences according to Fisher's least significant difference $p < 0.001$.

Table 4
Color differences ΔE* between the individual products where a small ΔE* value implies that the colors are close to each other (Pathare et al.,; 2013).

Pairwise ΔE*	Soy I	Soy II	Pea I
Soy II	5.1		
Pea I	1.2	4.4	
Pea II	8.8	12.3	9.9

By comparing the results presented in Tables 3 and 4, with previous results from cooked beef patties (L* 45.2; a* 4.0; b* 39.7) (Sakai et al., 2022) Pea II was found to exhibit the closest color characteristic in terms of lightness and yellowness. However, the redness of the product was higher compared to the real beef product indicated by the higher a* and lower Hue angle (Girolami et al., 2013). A higher redness in plant-based burger patties compared to real beef has been previously reported by Zhou et al. (2022) and could be the result of added red beet powder (see Table 1) or other coloring agents (Fernández-López et al., 2023; Wu et al., 2024). While the addition of coloring, which achieves a more meat-like color, is generally appreciated by consumers (Giacalone et al., 2022; Sogari et al., 2023), there is a lack of information regarding the extent to which it is perceived as positive. Kim et al. (2024) observed that consumers desired a brown color on their ideal plant-based meat alternatives. However, this may be related to the fact that consumers evaluated cooked products and is consistent with the status of cooked meat, given that uncooked fresh meat changes in color from red to brown when cooked (He et al., 2020).

Similar to the color, the projected particle area is important to characterize the visual appearance of the products. Thereby, as the analysis was based on 2D top-view images, depth information and potential overlapping of particles were not captured. Therefore, the results should be interpreted as surface-based particle dimensions rather than full 3D particle size. Based on the results presented in Fig. 2, Pea II and Soy I showed on average the largest pieces (no significant differences between the samples). However, Pea II (29 ± 56 mm^2) showed a large variation around the mean indicating a less homogenous product. In contrast, Soy II (12 ± 14 mm^2) contained the smallest pieces and the lowest variation in size.

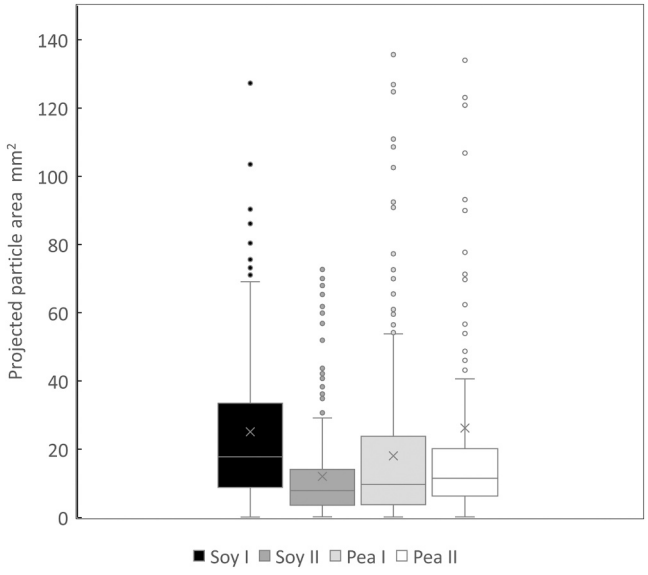

Fig. 2. Boxplot illustrating the projected particle area of the different products where × indicates the average of the data set that was used for statistical analysis ($p < 0.001$***; n.s. no significant difference). The middle bar represents the median, the edges of the box mark the interquartile range, the whiskers extend to the smallest and largest data points, and any points beyond the whiskers are considered outliers.

Similar sizes have been reported for mushroom-legume-based mince meat analogs (Mazumder et al., 2023). Considering that Pea II was the only product without pre-defined particles, the larger variation in particle size likely resulted from the uncontrolled formation and cutting of the matrix during production. This indicates that the particle size of such products could potentially be adjusted according to consumer preferences. The size of the other products is determined by the producer and cannot be altered during the cooking process. Although the particle size of the products differs significantly from one another there is at present no research available on what particle size is preferred by the consumers in the context of minced meat analogs.

3.4. Fiber orientation

Fiber orientation plays an important role in eliciting the perception of a meaty texture (Y. M. Choi & Kim, 2009; Ertbjerg & Puolanne, 2017). The structure obtained from the Light micrographs (LM), (Fig. 3) showed a more dominant fibrous structure for both Soy I and Pea I whereas Soy II and Pea II exhibited fewer fibers. While the fibers in Soy I are oriented in the same direction the fibers in Pea I showed more fibre bundles that oriented in different directions.

From the micrographs, the fiber orientation was determined using image analysis (see Figure A2 and A3 in appendix) (Rezakhaniha et al., 2012). Based on the image analysis (Table 5 and Figure A3) Soy I showed that most fibers (93 %) orientated in the same direction (between −90° and 0°) which is supported by the structure shown in Fig. 3A. In contrast, Pea I, Soy II, and Pea II showed a less homogeneous orientation with large numbers of fibers oriented between −90° and 90°.

Table 5
Quantitative results from the 2D fiber orientation analysis of meat analogue samples. The values represent the proportion (%) of fibers oriented within the specified angular ranges, determined from light microscopy micrographs using the OrientationJ plugin (Rezakhaniha et al.,; 2012). Higher values indicate a greater proportion of fibers aligned in a similar direction, reflecting increased anisotropy. A visual overview of the corresponding fiber orientation distributions is provided in Figure A2.

Product	Fiber orientation				Total
	-90° – 0°	%	0° – 90°	%	
Soy I	1 331 627	93	99 572	7	1 431 199
Soy II	335 457	43	446 863	57	782 320
Pea I	388 408	39	619 993	61	1 008 401
Pea II	293 059	35	542 664	65	835 723

This indicates that although Pea I showed a fibrous structure (Fig. 3C) the orientation of the fibers is more heterogeneous compared to the two soy products.

Previously presented results characterize the fibrous structure of meat analogues made from mung bean, soy, and pea protein using 2D images, demonstrating a strong correlation with expert panel evaluations (Ma et al., 2024). However, those studies examined products manufactured using high-temperature shear cell (HTSC) technology, which generates homogeneously aligned *macro-scale* fibres (Wu et al., 2024). In contrast, the present study focuses on the *microstructure* of minced-type meat analogues, where fibres and fibre bundles are much smaller and randomly distributed (Tornberg, 2005). Thus, the fibre characterisations based on 2D micrographs are largely influenced by the

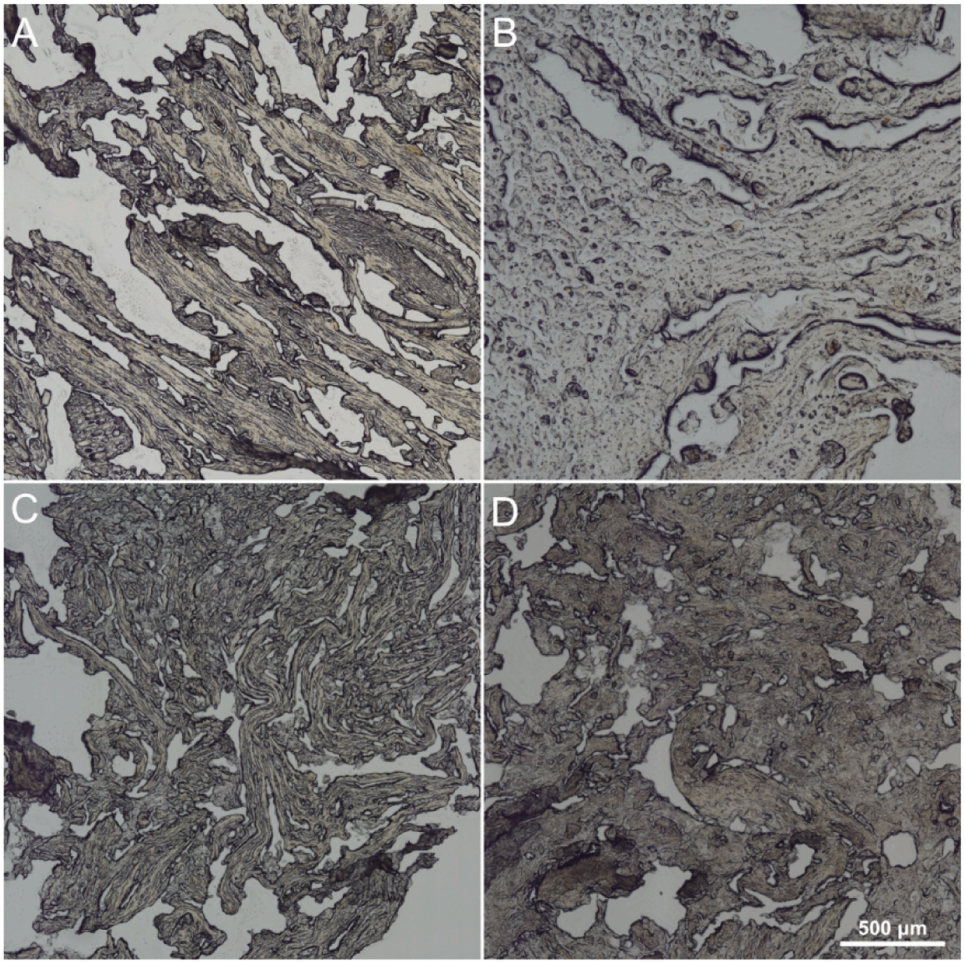

Fig. 3. Micrographs of the different products after cryosectioning (25µm); A: Soy I; B: Soy II; C: Pea I; D: Pea II used to determine the fiber distribution.

sample fixation during the cryo sectioning. Depending on the placement of the samples, as well as the sectioned region, the overall structure of the sample can vary. Therefore, 3D characterization using micro-CT and image analyses VGStudio Max – fiber composite analysis was used to avoid the potential error of false sample placement. The results of the fiber orientation of the 3D volumes are shown in Fig. 4 and Table 6. Therby fiber refers to the structural anisotropy observed in the 3D reconstructions, which reflects the alignment of material density within the product. In X-ray micro-CT imaging of plant-based meat analogues, regions of varying density (rather than actual protein fibers) are used to identify fibrous structures, as these correspond to the aligned protein and air-channel network formed during extrusion. Thus, the "fibers" visualized in our analysis represent the orientation of elongated, anisotropic features (including both proteinrich and void regions) that together define the fibrous texture of the samples. The main orientation tensor (Table 6) describes the fiber configuration inside the volume in the three directions xx, yy, and zz and adds up to 1 (Žirgulis et al., 2016). Based on these results, it is evident that the fibers present in all samples are isotropic (Medeghini et al., 2022) with fibers showing no preferred orientation.

The plane projections (Fig. 4, column IV) illustrate the distribution of fiber orientation. Overall, all samples show an isotropic fiber structure (Medeghini et al., 2022), indicating no pronounced directional alignment. However, soy II (Fig. 4B) exhibits a slightly higher density of fibers oriented between 270° and 0°, suggesting minor directional organization compared with the other samples. It should be noted that the absolute fiber orientation angles (e.g., −90° to 0°) depend on how the sample is positioned during imaging, both in 2D and 3D analyses. Therefore, the specific degree values are not directly comparable between samples; rather, the key parameter is the degree of alignment e.g. how many fibers are oriented in the same direction. A higher proportion of parallel fibers indicates a more anisotropic structure, which is typically associated with a firmer and more meat-like texture.

Based on the results from the space orientation (Fig. 4, IV), both Soy II and Pea I, show larger amounts of fiber bundles orientated in the same direction. Regarding Soy II, the majority of the fiber clusters are oriented at 270°–315°, whereas for Pea I, the majority of fiber clusters are oriented at 270°– 0°. Pea II shows a less homogeneous distribution with fibers mainly distributed between 0° and 180° and with more individual fibers oriented in other directions than the clusters. Therefore, it can be expected that Soy II would be perceived as more fibrous than the other products.

Further, previously presented results on fiber structures in meat analogs have suggested that more ordered fibrous structures can lead to firmer products (Lin et al., 2002). Thus, the higher hardness of Soy II could also be partially linked to the more ordered fibrous structure. The structure of the meat analog is dependent on numerous factors including the type of protein used for the texturizing process (Dekkers et al., 2018; Wang et al., 2022) as well as the processing parameters (Ferawati et al., 2021; Lin et al., 2002) making it difficult to predict.

When comparing the 2D and 3D imaging results, both methods revealed structural differences between the soy- and pea-based products, although the degree of fiber alignment varied depending on the technique used. The 2D light microscopy indicated more pronounced and directionally aligned fibers, particularly for Soy I and Pea I, whereas the 3D micro-CT analysis revealed a generally isotropic fiber distribution with only subtle preferential orientation in Soy II and Pea I. These differences likely arise from the distinct resolution, imaging principles, and contrast mechanisms of the two techniques. While the 2D method provides higher in-plane resolution and optical contrast that enhances the visibility of finer fibers at the surface level, the 3D micro-CT captures the entire sample volume at a lower voxel resolution, offering a more representative overview of the internal structure. In addition, the two datasets were processed using different image analysis tools, which may contribute to variations in how fibers and bundles were detected and quantified. Therefore, the observed differences between the 2D and 3D results can be attributed to both methodological and analytical differences rather than inconsistencies in the physical structure of the samples.

3.5. Consumer sensory evaluation

Table 7 presents the results of the hedonic evaluation of the samples. Consumers liked Soy II the most in terms of appearance ($p < 0.0001$) with a moderate effect size ($d = 0.6$), texture ($p = 0.003$) with a small effect size ($d = 0.3$), and overall ($p = 0.012$) with a small effect size ($d = 0.3$). In contrast, Soy I was least liked.

A statistically significant difference was observed in eleven of the fifteen sensory attributes concerning the appearance and texture modalities between the samples ($p < 0.008$, See Table 8). As observed in the TPA results presented in Section 3.1, a similar pattern was observed in the consumer sensory evaluation. The results indicated that Soy I and Soy II rated higher on chewing resistance than the pea products ($p < 0.0001$) with a moderate effect size ($d = 0.7$). Moreover, the soy products exhibited a higher rubbery texture than Pea I ($p < 0.0001$) with a moderate effect size ($d = 0.5$). Regarding the juicy and oily texture, which can be associated with the LHC results presented in Section 3.2, the consumer sensory evaluation showed that Pea II was perceived as the juiciest of the samples ($p < 0.0001$) with a moderate effect size ($d = 0.7$), while Pea I was perceived as the least oily ($p = 0.0003$) with a small effect size ($d = 0.4$). The results of the sensory evaluation and physicochemical analysis indicated that the observed patterns were comparable in terms of the appearance of the samples, particularly the color and size of pieces. As was the case with the color measurement results presented in Section 3.3, Pea II was observed as the reddest ($p < 0.0001$) with a large effect size ($d = 1.5$), while Soy II was rated the brownest ($p < 0.0001$) with a large effect size ($d = 1.2$) in the sensory evaluation. The results of the sensory evaluation indicated that consumers perceived the soy products to be more homogeneous in particle size than the pea products ($p < 0.0001$) with a moderate effect size ($d = 0.6$). This was similarly evident in the projected particle area presented in Section 3.4, particularly for Soy II and Pea II.

The sensory and physico-chemical data were further separately analyzed using PCA to model the samples in relation to each of the respective measurements (Fig. 5). In addition, the hedonic values were included as supplementary variables to PCA with sensory attributes (Fig. 5B) to indicate which characteristics could be related to product preference. The variance of the data for the physico-chemical attributes was explained by the first two factors, which explained 82 % of the variance. Similarly, the sensory attributes exhibited an 89 % variance explained by the first two factors. The PCA results demonstrated that the samples could be divided into two distinct clusters based on their physico-chemical and sensory characteristics. Soy I, Soy II, and Pea I were grouped together and characterized by physico-chemical properties such as 'Hardness', 'Gumminess', 'Chewiness', and 'Color_H*' (Fig. 5A). In contrast, Pea II was positioned on the opposite side, associated with 'Particle size', 'Color_C*', 'Color_L*', 'Color_a*', and 'Color_b*'. A similar pattern emerged for score projections when analyzed with the sensory attributes (Fig. 5B). Soy I, Soy II, and Pea I again clustered together, characterized by attributes such as 'Homogeneous pieces_AP', 'Homogeneous colour_AP', 'Brown colour_AP', 'Grainy_AP', and 'Grainy_TEX'. On the other hand, Pea II was situated on the opposite side, linked to 'Moist_AP', 'Red colour_AP', 'Juicy_TEX', 'Fibrous_AP', and 'Oily_TEX'.

The patterns of sample discrimination observed across sensory attributes were found to be similar to the physico-chemical analysis, albeit with some differences. Indeed, the overall consumer-driven sample configuration was found to align with the physico-chemical characteristics, as indicated by the MFA analysis (Fig. 6), wherein the first two factors accounted for 84 % of the variance. In the MFA loading plot (Fig. 6A) a strong correlation among the attributes related to color was observed, suggesting that the samples identified as vibrant or saturated

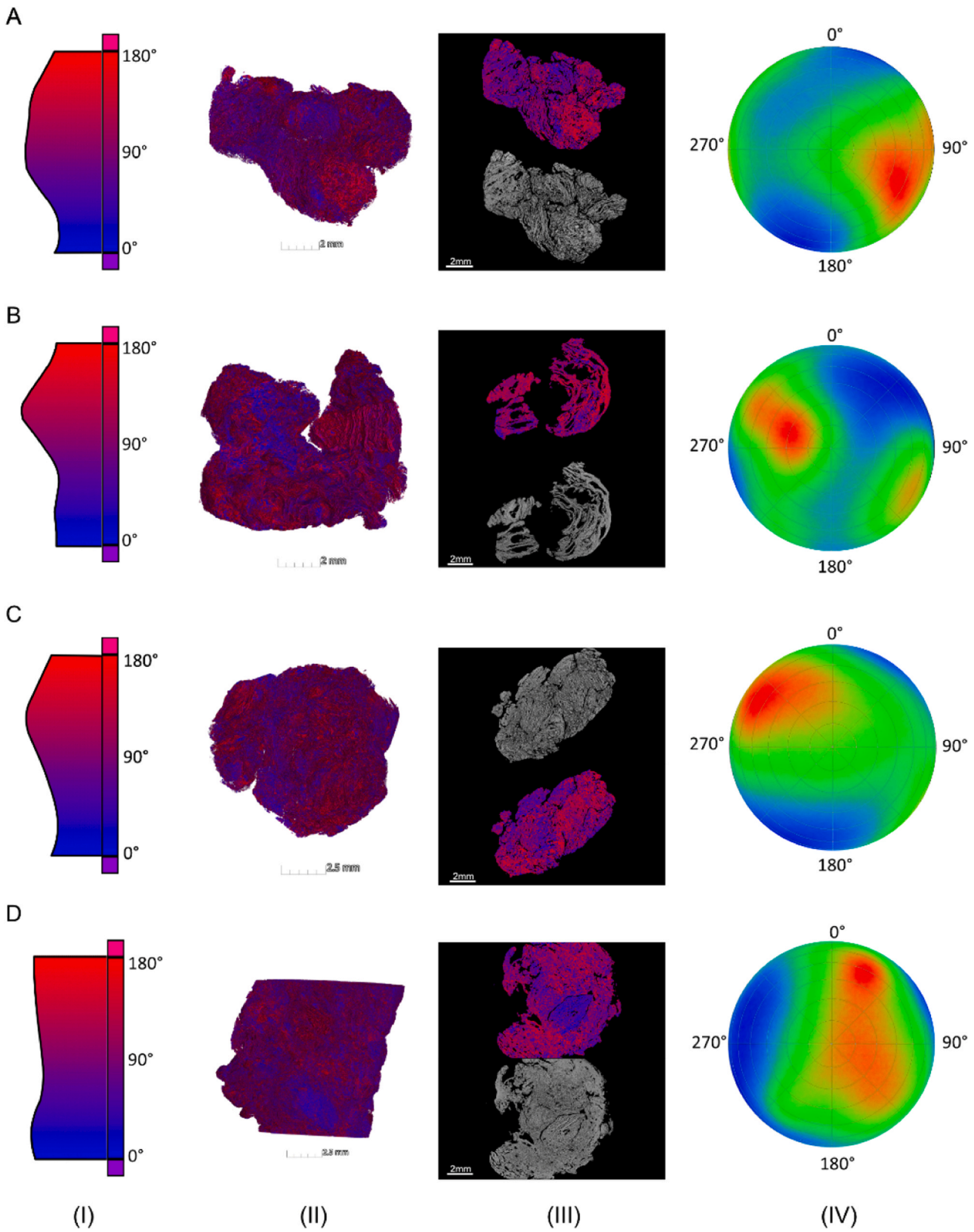

Fig. 4. Results from the fiber orientation analysis, including fiber distribution (I, II), CT reconstructions (III), and plane projection maps (IV) of the different products: A: Soy I; B: Soy II; C: Pea I; D: Pea II, using plane projection and space orientation analysis. The plane projections in Column IV illustrate the 2D visualization of fiber orientation distributions derived from the 3D datasets. The color gradient represents the degree of alignment, where red indicates regions with a high density of fibers aligned in a similar direction (fiber clusters), and green denotes more randomly oriented or isolated fibers. This visualization provides an overview of the uniformity and preferred orientation of fibers within each product.

Table 6
Overview of the main orientation tensor for xx, yy, and zz direction for all products.

Product	Mean orientation tensor		
	xx	yy	zz
Soy I	0.30	0.36	0.34
Soy II	0.32	0.34	0.34
Pea I	0.31	0.34	0.35
Pea II	0.34	0.31	0.35

Table 7
Mean liking scores (mean ± standard error) of the different meat analogs.

Products	Appearance	Texture	Overall
Soy I	5.31 ± 0.20^{b}	5.54 ± 0.20^{b}	5.44 ± 0.19^{b}
Soy II	6.80 ± 0.19^{a}	6.24 ± 0.21^{a}	6.20 ± 0.21^{a}
Pea I	6.74 ± 0.15^{a}	5.90 ± 0.19^{ab}	6.07 ± 0.18^{ab}
Pea II	6.15 ± 0.20^{a}	5.31 ± 0.21^{b}	5.85 ± 0.22^{ab}
P - value	< 0.0001	0.003	0.012
Cohen's *d*	0.6	0.3	0.3

Note: The hedonic scale was a 9-point scale. The different superscript letters indicate significant differences according to Kruskal-Wallis and post-hoc Dunn-Bonferroni tests ($p > 0.05$). Cohen's *d* interpretation was based on the following intervals: 0–0.1 (no effect), 0.2–0.4 (small effect), 0.5–0.7 (moderate effect), and 0.8 ≤ (large effect).

in physico-chemical color analysis were perceived similarly by consumers. Additionally, a negative correlation was observed between 'Particle size' and 'Homogeneous pieces_AP', indicating that larger particle sizes result in less visual homogeneity, leading to lower homogeneity scores from consumers and vice versa. Samples that released more fluid under low centrifugal force showed a similar vector direction to those for oily and juicy texture and moist appearance, as rated by consumers. This can be due to the release of loosely bound water and surface lipids under mild stress conditions, which may contribute to the perception of juiciness and moistness. In contrast, more tightly bound water, released only at higher centrifugal forces, is likely less relevant for sensory perception, as it remains entrapped within the matrix during normal consumption. Moreover, the physico-chemical measurements of hardness, chewiness, and gumminess showed a positive correlation with the consumer perception of chewing resistance. Hedonic value was employed as a supplementary variable in the MFA. It showed that texture liking was negatively related to the first factor. For instance, while 'Juicy_TEX' was positively correlated with the first factor, the inverse relationship observed with texture liking suggests that 'Juicy_TEX' may not be a major driver of texture preference. Furthermore, 'Grainy_TEX', which exhibited a negative correlation with the first factor, was not a preferred attribute among consumers. The consensus plot (Fig. 6B) confirmed that the physico-chemical analysis measurements aligned with consumer sensory perception. Furthermore, the closeness of the score projections was supported by the high RV coefficient (0.94). The coefficient ranges from 0 to 1, with values closer to 1 indicating greater similarity (Robert & Escoufier, 1976).

Pea II was sold refrigerated in stores, whereas the other products were sold frozen. This may have influenced the product's LHC and the fiber structure in terms of its isotropic distribution and heterogeneous orientation. Nevertheless, the consumer sensory evaluation indicated that the fibrous texture did not significantly differ across samples. However, consumers preferred the texture of Soy II, finding it chewier and more rubbery compared to the other products. This could indicate that more ordered fibrous structures in this type of product, as indicated in the 3D imaging results, are preferred by consumers. It also highlights the complexity of food texture and its perception. Further research is required to determine the point at which fiber orientation changes become noticeably different in perception by consumers and how this difference translates in terms of perceived textural quality and intensity. In addition, while Pea II exhibited greater juiciness compared to the other products and was perceived as a juicier product based on its LHC, the preference of texture was lower among the samples. Although juiciness has traditionally been considered as one of the distinctive qualities of meat products, it has been challenging to replicate this in meat analogs (Fiorentini et al., 2020). In the present study, juiciness was not the main influencer of texture preferences, which contradicts previous findings (Godschalk-Broers et al., 2022; Gonzalez-Estanol et al., 2023). Instead, a grainy texture was identified as a major source of consumer dislike in meat analogs. This particular aspect of texture has been previously linked to an undesirable mouthfeel in plant-based alternative products (Giacalone et al., 2022; Moss et al., 2023). This further emphasizes the importance of investigating the complex impact of sensory attributes on consumer acceptance (Fiorentini et al., 2020; Giacalone et al., 2022).

4. Limitations

This study employed various characterization methods that provide a comprehensive understanding of the attributes that consumers find most appealing in plant-based meat analogs. However, there are several limitations to this approach. Firstly, the lack of precise information regarding the composition of the samples, because they were obtained from commercial sources, constrained the capacity to ascertain the

Table 8
Mean of sensory attribute intensities (mean ± standard error) on different meat analogs.

Attributes	Soy I	Soy II	Pea I	Pea II	*P* - value	Cohen's D
Homogeneous pieces_AP	3.39 ± 0.12^{a}	3.41 ± 0.12^{a}	2.97 ± 0.11^{b}	2.62 ± 0.12^{b}	< 0.0001	0.6
Homogeneous colour_AP	4.27 ± 0.10	4.16 ± 0.11	4.15 ± 0.12	3.94 ± 0.12	0.137	0.2
Moist_AP	3.38 ± 0.11^{b}	3.07 ± 0.12^{bc}	2.99 ± 0.12^{c}	3.78 ± 0.11^{a}	< 0.0001	0.6
Brown colour_AP	3.03 ± 0.12^{bc}	4.27 ± 0.11^{a}	3.35 ± 0.11^{b}	2.63 ± 0.11^{c}	< 0.0001	1.2
Red colour_AP	2.08 ± 0.12^{b}	1.54 ± 0.09^{c}	2.32 ± 0.11^{b}	3.84 ± 0.11^{a}	< 0.0001	1.5
Grainy_AP	3.19 ± 0.14^{a}	3.20 ± 0.14^{a}	3.11 ± 0.13^{a}	2.44 ± 0.12^{b}	< 0.0001	0.5
Fibrous_AP	1.96 ± 0.12	2.07 ± 0.12	1.95 ± 0.12	2.16 ± 0.12	0.470	0.1
Chewing resistance_TEX	3.15 ± 0.10^{a}	3.36 ± 0.12^{a}	2.65 ± 0.11^{b}	2.60 ± 0.11^{b}	< 0.0001	0.7
Rubbery_TEX	2.89 ± 0.13^{a}	2.90 ± 0.14^{a}	2.16 ± 0.12^{b}	2.45 ± 0.13^{ab}	< 0.0001	0.5
Juicy_TEX	3.26 ± 0.13^{b}	3.02 ± 0.12^{b}	3.10 ± 0.13^{b}	3.95 ± 0.11^{a}	< 0.0001	0.7
Oily_TEX	2.83 ± 0.14^{a}	2.49 ± 0.13^{ab}	2.23 ± 0.12^{b}	2.96 ± 0.13^{a}	0.0003	0.4
Grainy_TEX	2.86 ± 0.14^{a}	2.94 ± 0.14^{a}	2.95 ± 0.13^{a}	2.29 ± 0.12^{b}	0.001	0.4
Mealy_TEX	1.82 ± 0.12^{ab}	1.70 ± 0.11^{b}	2.24 ± 0.13^{a}	1.77 ± 0.12^{b}	0.008	0.3
Remaining-after_TEX	2.28 ± 0.13	2.34 ± 0.14	2.45 ± 0.13	2.26 ± 0.13	0.630	0.1
Fibrous_TEX	2.00 ± 0.12	2.21 ± 0.13	1.97 ± 0.12	2.22 ± 0.13	0.340	0.1

Note: The scale for sensory attribute intensity was a 5-point scale. The different superscript letters indicate significant differences according to Kruskal-Wallis and post-hoc Dunn-Bonferroni tests ($p > 0.05$). Cohen's *d* interpretation is based on the following intervals: 0–0.1 (no effect), 0.2–0.4 (small effect), 0.5–0.7 (moderate effect), and 0.8 ≤ (large effect).

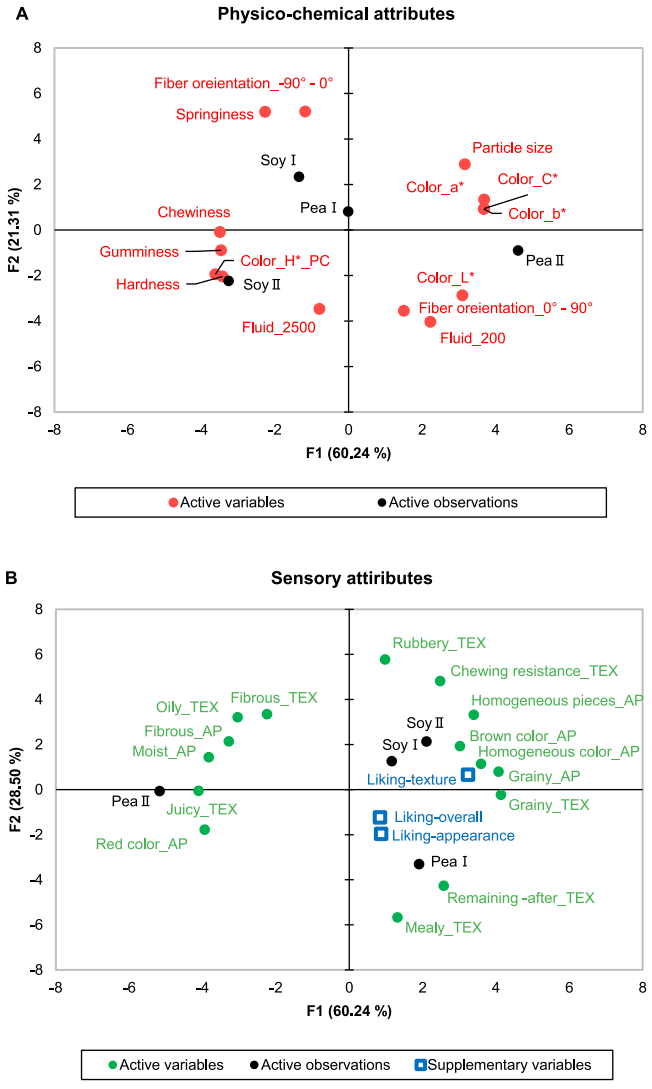

Fig. 5. The PCA biplots of physico-chemical attributes (A) and sensory attributes (B). *Note*: AP = appearance; TEX =texture; supplementary variables = hedonic attributes.

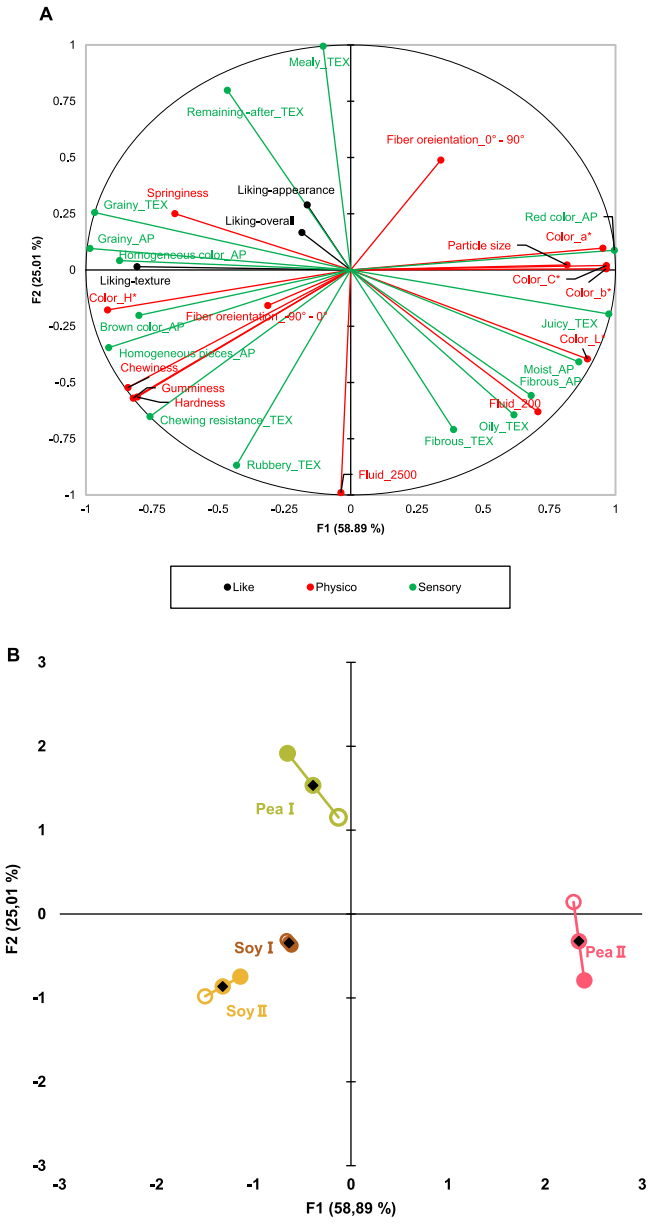

Fig. 6. The MFA loadings plot (A) and consensus plot (B) by physico-chemical and sensory modalities. Note: open circle = physico-chemical modalities; filled circle = sensory modalities; filled circle with black center = average of physico-chemical and sensory modalities projection.

extent to which specific ingredients impacted the texture of the product. Secondly, since no standardized method currently exists to measure the texture profile of minced meat, comparing the results obtained from this study with those from past and future studies remains challenging. Thirdly, characterizing fiber orientation in 2D food structures is limited. This is primarily due to the difficulty in obtaining a representative 2D section from a 3D object, as well as the fact that tools for fiber characterization are mainly designed for analyzing single fibers and their orientation. Although fiber characterization of 3D structures helps to address the issue of finding representative subvolumes by allowing the characterization of larger 3D volumes, the challenge remains because these applications are predominantly developed for and used in other structures, such as fiber-reinforced polymers. Lastly, it is important to note that the interpretation of sensory results based solely on the grand mean has its limitations, as consumer preferences are not homogeneous and can vary across different segments. Consequently, these findings should be interpreted with caution, as they do not fully capture the complexity of hedonics within the population.

5. Conclusion

This study aimed to identify the properties of plant-based minced meat analogs that are appreciated the most by consumers and should therefore be prioritized in further development. Various characterization methods were explored, including the potential application of fiber characterization tools. The results indicated that characterizing heterogeneous structures such as minced meat analogs is challenging, particularly because of the importance of sample orientation during cryosectioning. Utilizing 3D characterization methods, such as CT, can mitigate this issue and provide detailed insights into heterogeneous structures.

A strong alignment was found between physico-chemical properties (TPA, LHC, color measurement) and consumer sensory perception, with consumers demonstrating a similar ability to discriminate between the products. The products that exhibited certain textural and physiochemical properties – mechanically measured and described by consumers as chewy and gummy – were found to be more favoured among consumers. However, the presence of a grainy texture appeared to be

one of the major factors contributing to reduced consumer appreciation. Further investigation is needed to understand the complexity of sensory attributes that influence consumer acceptance and the extent to which consumers can perceive specific attributes, such as fiber structures.

CRediT authorship contribution statement

Mihaela Mihnea: Writing – review & editing, Conceptualization. **Sarah Heupl:** Writing – review & editing, Visualization, Formal analysis. **Jun Niimi:** Writing – review & editing, Supervision, Resources, Methodology, Funding acquisition, Conceptualization. **Åsa Öström:** Writing – review & editing, Supervision, Funding acquisition, Conceptualization. **Maud Langton:** Writing – review & editing, Supervision, Resources, Funding acquisition, Conceptualization. **Ansung Kim:** Writing – review & editing, Writing – original draft, Visualization, Validation, Methodology, Investigation, Formal analysis, Data curation, Conceptualization. **Jaqueline Auer:** Writing – review & editing, Writing – original draft, Visualization, Validation, Methodology, Investigation, Formal analysis, Data curation, Conceptualization.

Declaration of Competing Interest

We declare that the research was conducted in the absence of any financial relationships that could be construed as a potential conflict of interest.

Acknowledgements

This research was funded by a FORMAS grant for the project 'Plant-based proteins for health and wellbeing', PAN SWEDEN (2020–02843). Moreover, this study was financially supported by Trees and Crops for the Future (TC4F), a Strategic Research Area at SLU, supported by the Swedish Government.

Appendix A. Supporting information

Supplementary data associated with this article can be found in the online version at doi:10.1016/j.foostr.2025.100492.

Data Availability

Data will be made available on request.

References

Aaslyng, M. D., Bejerholm, C., Ertbjerg, P., Bertram, H. C., & Andersen, H. J. (2003). Cooking loss and juiciness of pork in relation to raw meat quality and cooking procedure. *Food Quality and Preference, 14*(4), 277–288. https://doi.org/10.1016/S0950-3293(02)00086-1

Adekunte, A. O., Tiwari, B. K., Cullen, P. J., Scannell, A. G. M., & O'Donnell, C. P. (2010). Effect of sonication on colour, ascorbic acid and yeast inactivation in tomato juice. *Food Chemistry, 122*(3), 500–507. https://doi.org/10.1016/j.foodchem.2010.01.026

Bakhsh, A., Lee, S. J., Lee, E. Y., Sabikun, N., Hwang, Y. H., & Joo, S. T. (2021). A novel approach for tuning the physicochemical, textural, and sensory characteristics of plant-based meat analogs with different levels of methylcellulose concentration. *Foods, 10*(3). https://doi.org/10.3390/foods10030560

Bourne, M. C. (1978). Texture profile analysis. *Food Technology, 32*, 62–66.

Candogan, K., & Kolsarici, N. (2003). The effects of carrageenan and pectin on some quality characteristics of low-fat beef frankfurters. *Meat Science, 64*(2), 199–206. https://doi.org/10.1016/S0309-1740(02)00181-X

Choi, Y. M., & Kim, B. C. (2009). Muscle fiber characteristics, myofibrillar protein isoforms, and meat quality. *Livestock Science, 122*(2–3), 105–118. https://doi.org/10.1016/j.livsci.2008.08.015

Choi, Y. S., Choi, J. H., Han, D. J., Kim, H. Y., Lee, M. A., Kim, H. W., Jeong, J. Y., & Kim, C. J. (2011). Effects of rice bran fiber on heat-induced gel prepared with pork salt-soluble meat proteins in model system. *Meat Science, 88*(1), 59–66. https://doi.org/10.1016/j.meatsci.2010.12.003

Damez, J. L., & Clerjon, S. (2008). Meat quality assessment using biophysical methods related to meat structure. *Meat Science, 80*(1), 132–149. https://doi.org/10.1016/j.meatsci.2008.05.039

Dekkers, B. L., Boom, R. M., & van der Goot, A. J. (2018). Structuring processes for meat analogues. *Trends in Food Science and Technology, 81*, 25–36. https://doi.org/10.1016/j.tifs.2018.08.011

Ertbjerg, P., & Puolanne, E. (2017). Muscle structure, sarcomere length and influences on meat quality: A review. *Meat Science, 132*, 139–152. https://doi.org/10.1016/j.meatsci.2017.04.261

Fehér, A., Gazdecki, M., Véha, M., Szakály, M., & Szakály, Z. (2020). A comprehensive review of the benefits of and the barriers to the switch to a plant-based diet. *Sustainability, 12*(10), 1–18. https://doi.org/10.3390/su12104136

Ferawati, F., Zahari, I., Barman, M., Hefni, M., Ahlström, C., Witthöft, C., & Östbring, K. (2021). High-moisture meat analogues produced from yellow pea and faba bean protein isolates/concentrate: Effect of raw material composition and extrusion parameters on texture properties. *Foods, 10*(4). https://doi.org/10.3390/foods10040843

Fernández-López, J., Ponce-Martínez, A. J., Rodríguez-Párraga, J., Solivella-Poveda, A. M., Fernández-López, J. A., Viuda -Martos, M., & Pérez-Alvarez, J. A. (2023). Beetroot juices as colorant in plant-based minced meat analogues: Color, betalain composition and antioxidant activity as affected by juice type. *Food Bioscience, 56*(September). https://doi.org/10.1016/j.fbio.2023.103156

Fiorentini, M., Kinchla, A. J., & Nolden, A. A. (2020). Role of sensory evaluation in consumer acceptance of plant-based meat analogs and meat extenders: A scoping review. *Foods, 9*(9). https://doi.org/10.3390/foods9091334

Fu, J., Sun, C., Chang, Y., Li, S., Zhang, Y., & Fang, Y. (2023). Structure analysis and quality evaluation of plant-based meat analogs. *Journal of Texture Studies, 54*(3), 383–393. https://doi.org/10.1111/jtxs.12705

Giacalone, D., Clausen, M. P., & Jaeger, S. R. (2022). Understanding barriers to consumption of plant-based foods and beverages: Insights from sensory and consumer science. *Current Opinion in Food Science, 48*, Article 100919. https://doi.org/10.1016/j.cofs.2022.100919

Girolami, A., Napolitano, F., Faraone, D., & Braghieri, A. (2013). Measurement of meat color using a computer vision system. *Meat Science, 93*(1), 111–118. https://doi.org/10.1016/j.meatsci.2012.08.010

Godschalk-Broers, L., Sala, G., & Scholten, E. (2022). Meat analogues: Relating structure to texture and sensory perception. *Foods, 11*(15). https://doi.org/10.3390/foods11152227

Gonzalez-Estanol, K., Orr, R. E., Hort, J., & Stieger, M. (2023). Can flavour and texture defects of plant-based burger patties be mitigated by combining them with a bun and tomato sauce? *Food Quality and Preference, 109*, Article 104920. https://doi.org/10.1016/j.foodqual.2023.104920

Grossmann, L., Kinchla, A. J., Nolden, A., & McClements, D. J. (2021). Standardized methods for testing the quality attributes of plant-based foods: Milk and cream alternatives. *Comprehensive Reviews in Food Science and Food Safety, 20*(2), 2206–2233. https://doi.org/10.1111/1541-4337.12718

Guyony, V., Fayolle, F., & Jury, V. (2022). High moisture extrusion of vegetable proteins for making fibrous meat analogs: A review. *Food Reviews International, 00*(00), 1–26. https://doi.org/10.1080/87559129.2021.2023816

He, J., Evans, N. M., Liu, H., & Shao, S. (2020). A review of research on plant-based meat alternatives: Driving forces, history, manufacturing, and consumer attitudes. *Comprehensive Reviews in Food Science and Food Safety, 19*(5), 2639–2656. https://doi.org/10.1111/1541-4337.12610

Hoek, A. C., Luning, P. A., Weijzen, P., Engels, W., Kok, F. J., & de Graaf, C. (2011). Replacement of meat by meat substitutes. A survey on person- and product-related factors in consumer acceptance. *Appetite, 56*(3), 662–673. https://doi.org/10.1016/j.appet.2011.02.001

Kaleda, A., Talvistu, K., Vaikma, H., Tammik, M. L., Rosenvald, S., & Vilu, R. (2021). Physicochemical, textural, and sensorial properties of fibrous meat analogs from oat-pea protein blends extruded at different moistures, temperatures, and screw speeds. *Future Foods, 4*, Article 100092. https://doi.org/10.1016/j.fufo.2021.100092

Kerslake, E., Kemper, J. A., & Conroy, D. (2022). What's your beef with meat substitutes? Exploring barriers and facilitators for meat substitutes in omnivores, vegetarians, and vegans (Article) *Appetite, 170*, Article 105864. https://doi.org/10.1016/j.appet.2021.105864.

Kim, A., Öström, Å., Mihnea, M., & Niimi, J. (2024). Consumers' attachment to meat: Association between sensory properties and preferences for plant-based meat alternatives. *Food Quality and Preference, 116*(February). https://doi.org/10.1016/j.foodqual.2024.105134

Lam, A. C. Y., Karaca, A. C., Tyler, R. T., & Nickerson, M. T. (2018). Pea protein isolates: Structure, extraction, and functionality. *Food Reviews International, 34*(2), 126–147. https://doi.org/10.1080/87559129.2016.1242135

Lenhard, W., & Lenhard, A. (2022). Computation of effect sizes. *Psychometrica.* https://doi.org/10.13140/RG.2.2.17823.92329

Lin, S., Huff, H. E., & Hsieh, F. (2002). Extrusion process parameters, sensory characteristics, and structural properties of a high moisture soy protein meat analog. *Journal of Food Science, 67*(3), 1066–1072. https://doi.org/10.1111/j.1365-2621.2002.tb09454.x

Ma, Y., Schlangen, M., Potappel, J., Zhang, L., & van der Goot, A. J. (2024). Quantitative characterizations of visual fibrousness in meat analogues using automated image analysis. *Journal of Texture Studies, 55*(1), 1–12. https://doi.org/10.1111/jtxs.12806

Maurer, J., Salaberger, D., Jerabek, M., Fröhler, B., Kastner, J., & Major, Z. (2024). Fibre and failure characterization in long glass fibre reinforced polypropylene by X-ray computed tomography. *Polymer Testing, 130*. https://doi.org/10.1016/j.polymertesting.2023.108313

Mazumder, M. A. R., Sukchot, S., Phonphimai, P., Ketnawa, S., Chaijan, M., Grossmann, L., & Rawdkuen, S. (2023). Mushroom–legume-based minced meat: Physico-chemical and sensory properties. *Foods, 12*(11), 2094. https://doi.org/10.3390/foods12112094

McClements, D. J., Weiss, J., Kinchla, A. J., Nolden, A. A., & Grossmann, L. (2021). Methods for testing the quality attributes of plant-based foods: Meat-and processed-meat analogs. *Foods, 10*(2). https://doi.org/10.3390/foods10020260

Medeghini, F., Guhathakurta, J., Tiberti, G., Simon, S., Plizzari, G. A., & Mark, P. (2022). Steered fiber orientation: Correlating orientation and residual tensile strength parameters of SFRC. *Materials and Structures/Materiaux et Constructions, 55*(10). https://doi.org/10.1617/s11527-022-02082-9

Michel, F., Hartmann, C., & Siegrist, M. (2021). Consumers' associations, perceptions and acceptance of meat and plant-based meat alternatives (Article) *Food Quality and Preference, 87*, Article 104063. https://doi.org/10.1016/j.foodqual.2020.104063.

Mikael Furu. (2020). *Marknadsanalys och potential för växtbaserade proteiner Rapport till Anna Pers och Amanda Andersson, LRF: Vol. Januari.* ⟨https://www.vaxtbaseratsverige.se/uploads/2020/10/Så-blir-Sverige-världsledande-på-växtbaserat-rapport-från-Växbaserat-Sverige-20201015.pdf⟩.

Moss, R., LeBlanc, J., Gorman, M., Ritchie, C., Duizer, L., & McSweeney, M. B. (2023). A prospective review of the sensory properties of plant-based dairy and meat alternatives with a focus on texture. *Foods, 12*(8), 1709. https://doi-org.db.ub.oru.se/10.3390/foods12081709.

Niimi, J., Sörensen, V., Mihnea, M., Valentin, D., Bergman, P., & Collier, E. S. (2022). Does cooking ability affect consumer perception and appreciation of plant-based protein in Bolognese sauces? (Article) *Food Quality and Preference, 99*, Article 104563. https://doi.org/10.1016/j.foodqual.2022.104563.

Nishinari, K., & Fang, Y. (2018). Perception and measurement of food texture: Solid foods. *Journal of Texture Studies, 49*(2), 160–201. https://doi.org/10.1111/jtxs.12327

Özer, C. O., & Seçen, S. M. (2018). Effects of quinoa flour on lipid and protein oxidation in raw and cooked beef burger during long term frozen storage. *Food Science and Technology (Brazil), 38*, 221–227. https://doi.org/10.1590/fst.36417

Pathare, P. B., Opara, U. L., & Al-Said, F. A. J. (2013). Colour measurement and analysis in fresh and processed foods: A review. *Food and Bioprocess Technology, 6*(1), 36–60. https://doi.org/10.1007/s11947-012-0867-9

Ramos Diaz, J. M., Kantanen, K., Edelmann, J. M., Suhonen, H., Sontag-Strohm, T., Jouppila, K., & Piironen, V. (2022). Fibrous meat analogues containing oat fiber concentrate and pea protein isolate: Mechanical and physicochemical characterization. *Innovative Food Science and Emerging Technologies, 77*, Article 102954. https://doi.org/10.1016/j.ifset.2022.102954

Rezakhaniha, R., Agianniotis, A., Schrauwen, J. T. C., Griffa, A., Sage, D., Bouten, C. V. C., Van De Vosse, F. N., Unser, M., & Stergiopulos, N. (2012). Experimental investigation of collagen waviness and orientation in the arterial adventitia using confocal laser scanning microscopy. *Biomechanics and Modeling in Mechanobiology, 11*(3–4), 461–473. https://doi.org/10.1007/s10237-011-0325-z

Robert, P., & Escoufier, Y. (1976). *A Unifying Tool for Linear Multivariate Statistical Methods: The RV- Coefficient. Applied Statistics, 25*(3), 257–265. https://doi.org/10.2307/2347233.

Sakai, K., Sato, Y., Okada, M., & Yamaguchi, S. (2022). Synergistic effects of laccase and pectin on the color changes and functional properties of meat analogs containing beet red pigment. *Scientific Reports, 12*(1), 1–10. https://doi.org/10.1038/s41598-022-05091-4

Satija, A., & Hu, F. B. (2018). Plant-based diets and cardiovascular health. *Trends in Cardiovascular Medicine, 28*(7), 437–441. https://doi.org/10.1016/j.tcm.2018.02.004

Schoeman, L., Williams, P., du Plessis, A., & Manley, M. (2016). X-ray micro-computed tomography (μCT) for non-destructive characterisation of food microstructure. *Trends in Food Science Technology, 47*, 10–24. https://doi.org/10.1016/j.tifs.2015.10.016

Schreuders, F. K. G., Dekkers, B. L., Bodnár, I., Erni, P., Boom, R. M., & van der Goot, A. J. (2019). Comparing structuring potential of pea and soy protein with gluten for meat analogue preparation. *Journal of Food Engineering, 261*, 32–39. https://doi.org/10.1016/j.jfoodeng.2019.04.022

Schreuders, F. K. G., Schlangen, M., Kyriakopoulou, K., Boom, R. M., & van der Goot, A. J. (2021). Texture methods for evaluating meat and meat analogue structures: A review. *Food Control, 127*, Article 108103. https://doi.org/10.1016/j.foodcont.2021.108103

Sogari, G., Caputo, V., Joshua Petterson, A., Mora, C., & Boukid, F. (2023). A sensory study on consumer valuation for plant-based meat alternatives: What is liked and disliked the most? *Food Research International, 169*, Article 112813. https://doi.org/10.1016/j.foodres.2023.112813

Tornberg, E. (2005). Effects of heat on meat proteins - Implications on structure and quality of meat products. *Meat Science, 70*(3 SPEC. ISS.), 493–508. https://doi.org/10.1016/j.meatsci.2004.11.021

Wang, H., van den Berg, F. W. J., Zhang, W., Czaja, T. P., Zhang, L., Jespersen, B. M., & Lametsch, R. (2022). Differences in physicochemical properties of high-moisture extrudates prepared from soy and pea protein isolates. *Food Hydrocolloids, 128* (January), 0–9. https://doi.org/10.1016/j.foodhyd.2022.107540

Wi, G., Bae, J., Kim, H., Cho, Y., & Choi, M.-J. (2020). Evaluation of the physicochemical and structural properties and the sensory characteristics of meat analogues prepared with various non-animal based liquid additives. *Foods, 9*(4), 461. https://doi.org/10.3390/foods9040461

Wild, F. (2016). Manufacture of meat analogues through high moisture extrusion. *Reference Module in Food Science*. Elsevier. https://doi.org/10.1016/b978-0-08-100596-5.03281-9

Wilkinson, C., Dijksterhuis, G. B., & Minekus, M. (2000). From food structure to texture. *Trends in Food Science and Technology, 11*(12), 442–450. https://doi.org/10.1016/S0924-2244(01)00033-4

World Medical Association. (2013). World Medical Association Declaration of Helsinki: ethical principles for medical research involving human subjects. *JAMA, 310*(20), 2191–2194. https://doi.org/10.1001/jama.2013.281053

Wu, H., Sakai, K., Zhang, J., & Mcclements, D. J. (2024). Plant - based meat analogs: color challenges and coloring agents. *Food, Nutrition and Health, 1*, 19. https://doi.org/10.1007/s44403-024-00005-w

Xu, X., Sharma, P., Shu, S., Lin, T.-S., Ciais, P., Tubiello, F. N., Smith, P., Campbell, N., & Jain, A. K. (2021). Global greenhouse gas emissions from animal-based foods are twice those of plant-based foods. *Nature Food, 2*(9), 724–732. https://doi.org/10.1038/s43016-021-00358-x

Zhang, M., Mittal, G. S., & Barbut, S. (1995). Effects of test conditions on the water holding capacity of meat by a centrifugal method. *LWT - Food Science and Technology, 28*(1), 50–55. https://doi.org/10.1016/S0023-6438(95)80012-3

Zhou, B., & Uchida, Y. (2017). Influence of flowability, casting time and formwork geometry on fiber orientation and mechanical properties of UHPFRC. *Cement and Concrete Research, 95*, 164–177. https://doi.org/10.1016/j.cemconres.2017.02.017

Zhou, H., Vu, G., Gong, X., & McClements, D. J. (2022). Comparison of the cooking behaviors of meat and plant-based meat analogues: Appearance, texture, and fluid holding properties. *ACS Food Science and Technology, 2*(5), 844–851. https://doi.org/10.1021/acsfoodscitech.2c00016

Žirgulis, G., Švec, O., Sarmiento, E. V., Geiker, M. R., Cwirzen, A., & Kanstad, T. (2016). Importance of quantification of steel fibre orientation for residual flexural tensile strength in FRC. *Materials and Structures/Materiaux et Constructions, 49*(9), 3861–3877. https://doi.org/10.1617/s11527-015-0759-3